

Development of Compact Permanent Magnet Electron Focusing Device

Anirudh Rameshan

August 2023

1 Introduction

Table 1: Values of parameters of prototype magnets

	LLR01	LLR02	LLR03
Length (mm)	36	120	100
Bore Radius (mm)	3.5	9	15
Field Gradient (T/m)	222	94	57

2 Quadrupole Doublet: Point-Point to Parallel-Parallel Focusing

In this section (Maxima filename: *Doublets-PaPa-AR*), we study and compare the point-point to parallel-parallel focusing of two different quadrupole doublets:

1. LLR02 - LLR03
2. LLR01 - LLR03

Firstly, we specify the directories where we would like to load files from and where we wish to store our temporary data like plots. Then, we load the file *BeamOpticsLibrary-V1.0.wxm* which contains the definitions of the transport matrices that we would require in the study.

In the next step, we enter the values of the parameters of the magnets of the two doublets: their lengths, bore radii and field gradients. These values are stored in matrices such that the i^{th} row and the j^{th} column correspond to the i^{th} doublet and the i^{th} magnet from the beam source, respectively.

Now, we construct the transport matrix R for a general doublet using those of

drift and quadrupole. Since we are interested in point-point to parallel-parallel focusing, we have

$$\begin{pmatrix} x \\ 0 \\ y \\ 0 \end{pmatrix} = \begin{pmatrix} R_{11} & R_{12} & 0 & 0 \\ R_{21} & R_{22} & 0 & 0 \\ 0 & 0 & R_{33} & R_{34} \\ 0 & 0 & R_{43} & R_{44} \end{pmatrix} \begin{pmatrix} 0 \\ x'_0 \\ 0 \\ y'_0 \end{pmatrix}, \quad (1)$$

where the column matrices on the RHS and the LHS are respectively the initial and the final states of the electron, and the square matrix is the doublet transport matrix. This implies that

$$x = R_{12} x'_0 \quad (2)$$

and

$$y = R_{34} y'_0, \quad (3)$$

and the **condition for point-point to parallel-parallel focusing** is

$$R_{22} = R_{44} = 0. \quad (4)$$

Simultaneously solving these two equations for D_1 , the drift distance from the electron source to the first quadrupole, and D_2 , the drift distance between the two quadrupoles, we get two pairs of solutions. The values of the quadrupole parameters are substituted in them and the resulting expressions in momentum p of the electron are stored in a list Ddb of two matrices: the expression for D_k given by the j -th solution for the i -th doublet is $Ddb[i][j, k]$.

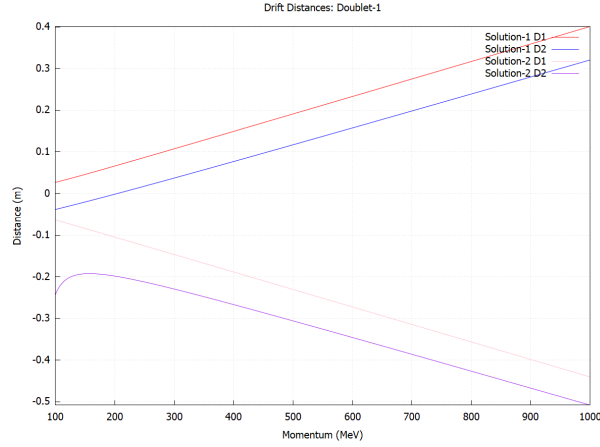


Figure 1: Drift distances: doublet-1

Next, we study the obtained solutions for each doublet by plotting them (Figure 1 and Figure 2). It is seen from the plots that only solution-1 gives positive real values of D_1 and D_2 in the momentum range of interest, 100–1000 MeV;

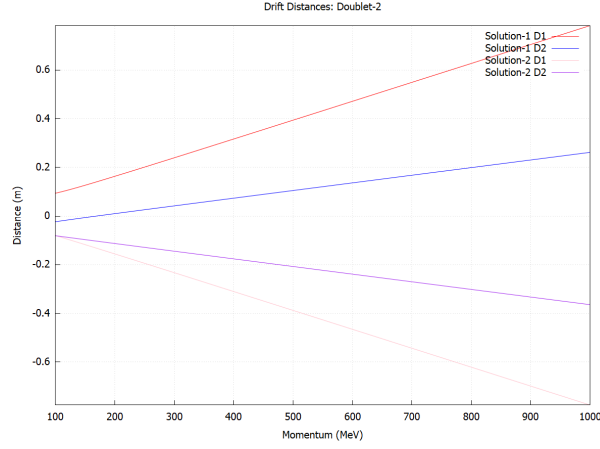



Figure 2: Drift distances: doublet-2

D_2 starts out negative, but quickly becomes positive. Both D_1 and D_2 increase with momentum. So, we require a longer system for focusing electrons of higher momentum. Solution does not cease to exist even for momentum values of the order of 10^4 MeV. In the domain of interest, the graphs look linear — but they are not, because of the trigonometric and the hyperbolic functions appearing in the quadrupole transfer matrix. It would be an interesting exercise to algebraically derive this linearity; a starting point would be to use the Taylor expansion of the functions involved and then try to show that the linear terms dominate. 

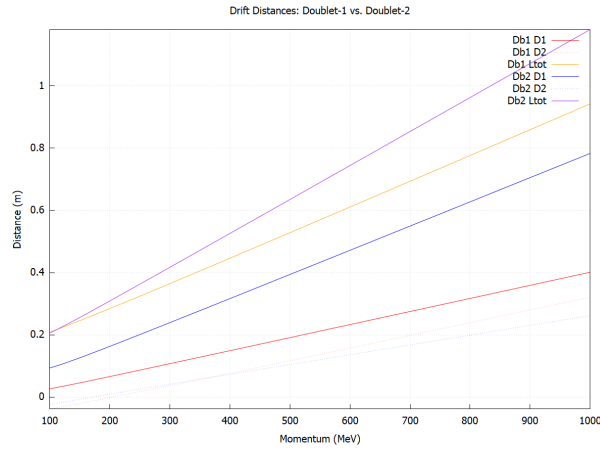


Figure 3: Drift distances: doublet-1 vs. doublet-2

On comparing the drift distances of the two doublets and the corresponding

total lengths (Figure 3), we find that Doublet-1 gives a shorter length in almost the entire domain despite the first magnet of Doublet-2 being shorter and having a higher field gradient.

Next, we study **beam size and aspect ratio**. From equations (2) and (3), for point-point to parallel-parallel focusing, the final position of the electron is given by $x = R_{12} x'_0$ and $y = R_{34} y'_0$. And, from equation (4), the condition for point-point to parallel-parallel focusing is $R_{22} = R_{44} = 0$. Also, the determinant of each of the two main-diagonal blocks is 1; therefore, $R_{12} = -1/R_{21}$ and $R_{34} = -1/R_{43}$. The expressions for R_{21} and R_{43} are simpler than those of R_{12} and R_{34} respectively. So, we could use these relations to simplify the calculation of beam size and aspect ratio. Thus, we have:

$$\text{Beam size along } x\text{-axis, } H_x = R_{12} x'_0 = -\frac{x'_0}{R_{21}} \quad (5)$$

$$\text{Beam size along } y\text{-axis, } H_y = R_{34} y'_0 = -\frac{y'_0}{R_{43}} \quad (6)$$

$$\text{Beam aspect ratio, } H_x/H_y = \frac{R_{12} x'_0}{R_{34} y'_0} = \frac{R_{43}}{R_{21}} \frac{x'_0}{y'_0} \quad (7)$$

The plots of these quantities for the two doublets are given below (Figure 4). The beam size increases and the beam aspect ratio decreases with momentum.

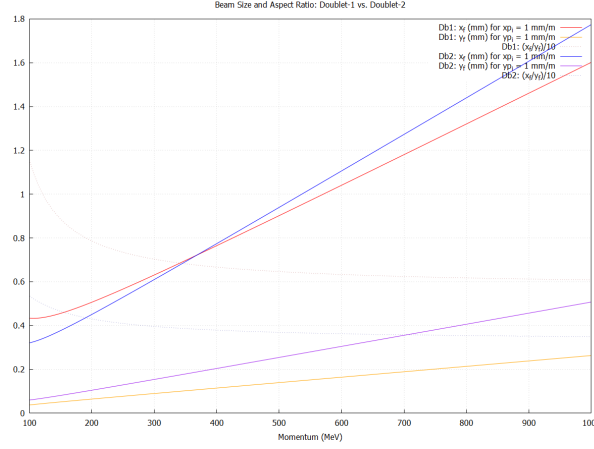


Figure 4: Beam size and aspect ratio: doublet-1 vs. doublet-2

This means that if $x'_0 = y'_0$, then the beam would be rounder for higher momenta. The rate of decrease in aspect ratio drops gradually with momentum.

The next quantity that is studied is the **angular acceptance** of the doublets for the electron beam and the laser. For simplicity, assume $x'_0 = y'_0 = \theta$. We need to find the maximum θ with which the beam passes through the quadrupole

magnets without touching their wall as a function of momentum p of the beam. To do this, we first assign θ some value, say $\theta_0 = 15$ mm/m. Then, we look for local maxima of x inside the first quadrupole magnet. We compare them and the values at the ends of the magnet to obtain the global maxima $x_{max} = x_0$. Now, since x scales linearly with θ everywhere (similar to equations 2), we can find the θ for which x_{max} is equal to the bore radius, R :

$$\theta_{max} = \frac{\theta_0}{x_0} R \quad (8)$$

Repeat the procedure for the second quadrupole magnet and compare the two θ_{max} s: the lesser of the two is the maximum θ in the x -direction. In the same way, we can find the maximum θ in the y -direction.

Obtaining the local maxima of x and y inside the magnets can be simplified by the following considerations. Consider an electron of momentum P and initial state $(X_0 \ X'_0 \ Y_0 \ Y'_0)^T$ entering a quadrupole magnet of length L and field gradient G . Let G be positive if the magnet is converging in x -direction and negative otherwise. The equation of motion of the electron is

$$\begin{pmatrix} X \\ X' \\ Y \\ Y' \end{pmatrix} = \begin{pmatrix} \cos(Kz) & \frac{\sin(Kz)}{K} & 0 & 0 \\ -K \sin(Kz) & \cos(Kz) & 0 & 0 \\ 0 & 0 & \cosh(Kz) & \frac{\sinh(Kz)}{K} \\ 0 & 0 & K \sinh(Kz) & \cosh(Kz) \end{pmatrix} \begin{pmatrix} X_0 \\ X'_0 \\ Y_0 \\ Y'_0 \end{pmatrix} \quad (9)$$

where $z \in [0, L]$ and $K = \sqrt{eG/P}$; K is real when G is positive and imaginary when G is negative.

At points of local extrema z_{0x} s of X , $X' = 0$. So,

$$-K \sin(Kz_{0x}) X_0 + \cos(Kz_{0x}) X'_0 = 0, \quad (10)$$

which gives

$$K \tan(Kz_{0x}) = \frac{X'_0}{X_0}, \quad X_0 \neq 0. \quad (11)$$

If $X_0 = 0$, we have

$$\cos(Kz_{0x}) X'_0 = 0, \quad (12)$$

which, if $X'_0 \neq 0$ and $K \in \mathbb{R}$, gives

$$z_{0x} = (2n - 1) \frac{\pi}{2K}, \quad n \in \mathbb{Z} \quad (13)$$

If K is imaginary, $\cos(Kz_{0x}) = \cosh(|K|z_{0x}) = 0$, which has no solution.

If $X_0 = 0$ and $X'_0 = 0$, the particle remains in the $X = 0$ plane.

Similarly, at points of local extrema z_{0y} s of Y , $Y' = 0$. So,

$$K \sinh(K z_{0y}) Y_0 + \cosh(K z_{0y}) Y'_0 = 0, \quad (14)$$

which gives

$$K \tanh(K z_{0y}) = -\frac{Y'_0}{Y_0}, \quad Y_0 \neq 0. \quad (15)$$

If $Y_0 = 0$, we have

$$\cosh(K z_{0y}) Y'_0 = 0, \quad (16)$$

which, if $Y'_0 \neq 0$ and $K \in \mathbb{R}$, has no solution. If K is imaginary, $\cosh(K z_{0y}) = \cos(|K| z_{0y}) = 0$, which gives the solution

$$z_{0y} = (2n - 1) \frac{\pi}{2K}, \quad n \in \mathbb{Z}. \quad (17)$$

If $Y_0 = 0$ and $Y'_0 = 0$, the particle remains in the $Y = 0$ plane.

For the $X_0 \neq 0$ and $Y_0 \neq 0$ cases, note that

- $\tan(\rho)$ is a periodic function when $\rho \in \mathbb{R}$. So, the equation $\tan(\rho) = r$, where r is a real constant, has infinitely-many solutions that differ from each other by an integral multiple of π . The principal solution (i.e. $\rho \in (-\pi/2, \pi/2)$) is zero if $r = 0$, positive if $r > 0$, and negative if $r < 0$.
- $\tanh(\rho)$ is a monotonously increasing function when $\rho \in \mathbb{R}$. It is bounded between -1 and 1. So, the equation $\tanh(\rho) = r$, where r is a real constant, has one solution if $|r| \leq 1$ and no solution if $|r| \geq 1$. In the former case, the solution is zero if $r = 0$, positive if $r > 0$, and negative if $r < 0$.
- $\tan(i\rho) = i \tanh(\rho)$ and $\tanh(i\rho) = i \tan(\rho)$ where $\rho \in \mathbb{R}$. So, the equations $i \tan(i\rho) = r$ and $i \tanh(i\rho) = r$, where $r \in \mathbb{R}$, may be written as $\tanh(\rho) = -r$ and $\tan(\rho) = -r$, respectively.

So, if $X'_0 = 0$, $z_{0x} = n\pi$, $n \in \mathbb{Z}$, for real K , and $z_{0x} = 0$ for imaginary K . Similarly, if $Y'_0 = 0$, $z_{0y} = 0$ for real K , and $z_{0y} = n\pi$, $n \in \mathbb{Z}$, for imaginary K . For $X'_0 \neq 0$ and $Y'_0 \neq 0$, the nature of the solutions of equations (11) and (15) for different possibilities of $(\alpha/|\alpha|, K/|K|)$ and $(\beta/|\beta|, K/|K|)$, where $\alpha = X'_0/X_0$ and $\beta = Y'_0/Y_0$, are as follows:

1. (1, 1)

(a) $K \tan(z_0 K) = X'_0/X_0$: Infinitely-many solutions with positive principal solution

$$z_{0x} = \tan^{-1}(X'_0/(K X_0))/K \quad (18)$$

(b) $K \tanh(z_0 K) = -Y'_0/Y_0$: One negative solution

$$z_{0y} = \tanh^{-1}(-Y'_0/(K Y_0))/K \quad (19)$$

if $Y'_0/(KY_0) \leq 1$.

2. $(-1, 1)$

(a) $K \tan(z_0 K) = X'_0/X_0$: Infinitely-many solutions with negative principal solution

$$z_{0x} = \tan^{-1}(X'_0/(KX_0))/K \quad (20)$$

(b) $K \tanh(z_0 K) = -Y'_0/Y_0$: One positive solution

$$z_{0y} = \tanh^{-1}(-Y'_0/(KY_0))/K \quad (21)$$

if $Y'_0/(KY_0) \leq 1$.

3. $(1, i)$

(a) $K \tan(z_0 K) = X'_0/X_0$: One negative solution

$$z_{0y} = \tanh^{-1}(-Y'_0/(KY_0))/K \quad (22)$$

if $Y'_0/(KY_0) \leq 1$.

(b) $K \tanh(z_0 K) = -Y'_0/Y_0$: Infinitely-many solutions with positive principal solution

$$z_{0x} = \tan^{-1}(X'_0/(KX_0))/K \quad (23)$$

4. $(-1, i)$

(a) $K \tan(z_0 K) = X'_0/X_0$: One positive solution

$$z_{0y} = \tanh^{-1}(-Y'_0/(KY_0))/K \quad (24)$$

if $Y'_0/(KY_0) \geq -1$.

(b) $K \tanh(z_0 K) = -Y'_0/Y_0$: Infinitely-many solutions with negative principal solution

$$z_{0x} = \tan^{-1}(X'_0/(KX_0))/K \quad (25)$$

Thus, we have considered at all the possible types of solutions of the equations (10) and (14). Note that only those solutions are relevant that lie in the interval $(0, L)$.

Obtaining the angular acceptance for the laser is simple. It is the angle subtended at the laser source by the center of the bore of the magnet and a point on the edge of the bore that is farther from the laser source. So,

$$\theta_{laser} = \tan^{-1} \left(\frac{R}{d} \right), \quad (26)$$

where R is the bore radius and d the distance from the laser source to the farther end of the magnet.

The plots of angular acceptance of the two doublets for the electron beam and the laser are given below (Figure 5).

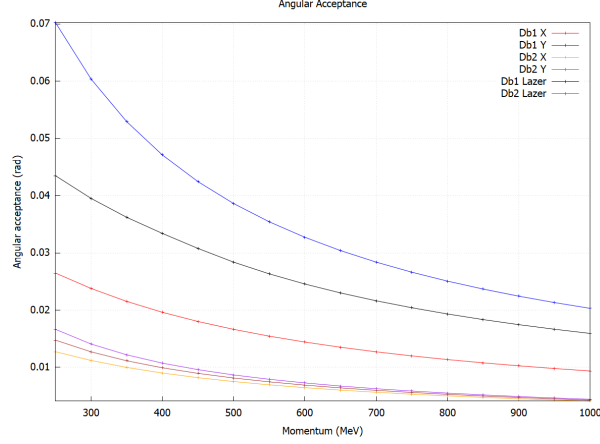


Figure 5: Angular Acceptance

The variation of angular acceptance is similar in all the plots. x -axis is the axis that limits the angular acceptance in both the doublets.

Finally, we trace the trajectory of an electron of a fixed momentum, say $p = 500$ MeV and initial divergence, say $x'_0 = -y'_0 = 15$ mm/m. For this, we define the trajectory in each section of the electron's path – drift - magnet - drift - magnet - drift – and then plot them together. The result is given in Figure 6.

It is clear from the plot that Doublet-2 is not suitable for the chosen values of momentum and divergences. This was expected from Figure 5.

3 Quadrupole Triplet: Point-Point to Parallel-Parallel Focusing

In this section (Maxima filename: Triplets2-PaPa-AR), we study and compare the point-point to parallel-parallel focusing of two different quadrupole triplets.

1. LLR01 - LLR02 - LLR03
2. (36,5.3,155) - (120,9,94) - (100,15,57)
where the triplet (l, r, g) represent a quadrupole magnet of length l mm, bore radius r mm and field gradient g T/m.

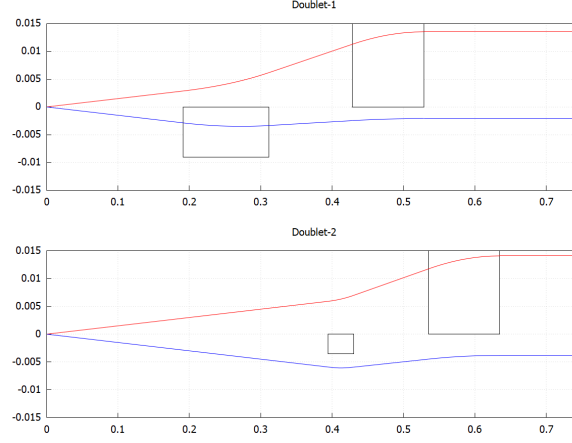


Figure 6: Electron trajectories for $p = 500$ MeV and $x'_0 = -y'_0 = 15$ mm/m

The method of study is same as that used for the quadrupole doublets in the previous section. First, we specify the relevant directories and load the required files. Then, the values of the parameters of the magnets are stored in matrices. Next, the general transport matrix R is constructed. The equations we need to solve are again $R_{22} = R_{44} = 0$. But, this time, we have three unknowns: (i) D_1 , the drift distance from the electron source to the first quadrupole, (ii) D_2 , that between the first and the second quadrupoles, and (iii) D_3 , that between the second and the third quadrupoles. Next, we solve the equations simultaneously for D_1, D_2 and D_3 . This gives four solutions. The values of the magnet parameters are substitutes in these solutions and they are store in a list of two matrices D_{tp} , like we did in the previous section. We observe that, in solutions 1 and 2, D_1 is a free parameter and D_2 and D_3 depend on D_1 , while in solutions 3 and 4, D_1, D_2 and D_3 are independent of each other. Next, we study the obtained solutions for each triplet by plotting them.

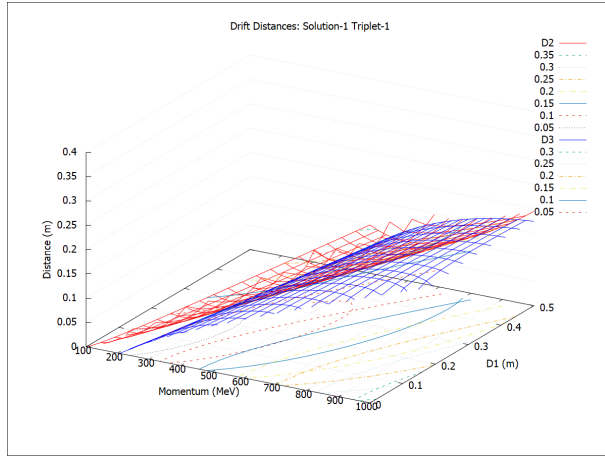


Figure 7: Drift distances: Solution-1, Triplet-1

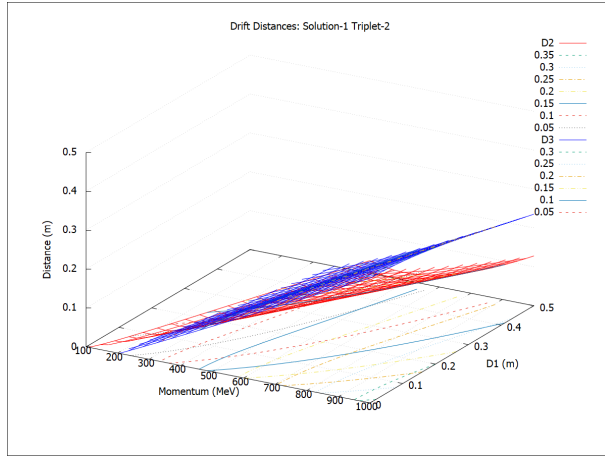


Figure 8: Drift distances: Solution-1, Triplet-2

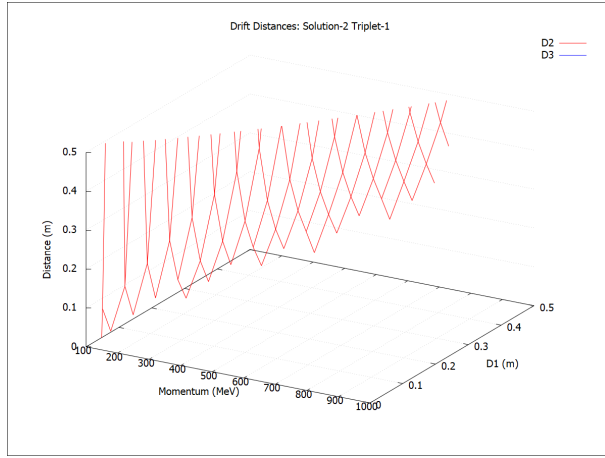


Figure 9: Drift distances: Solution-2, Triplet-1

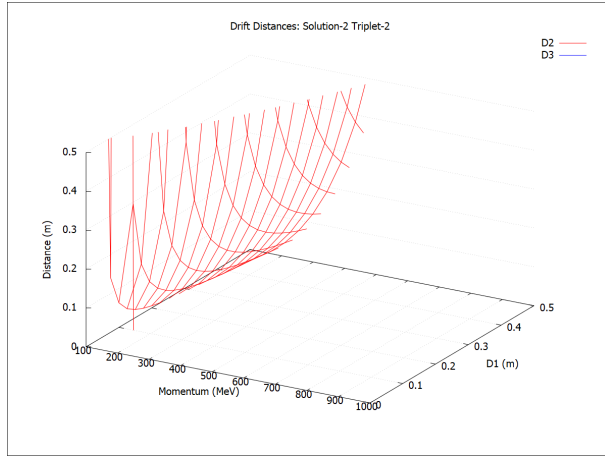


Figure 10: Drift distances: Solution-2, Triplet-2

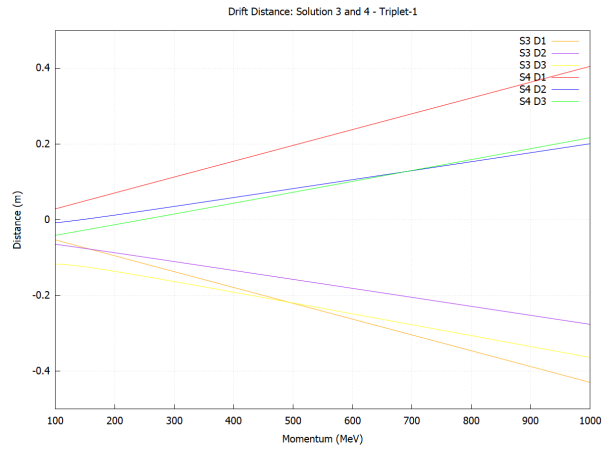


Figure 11: Drift distances: Solutions 3 & 4, Triplet-1

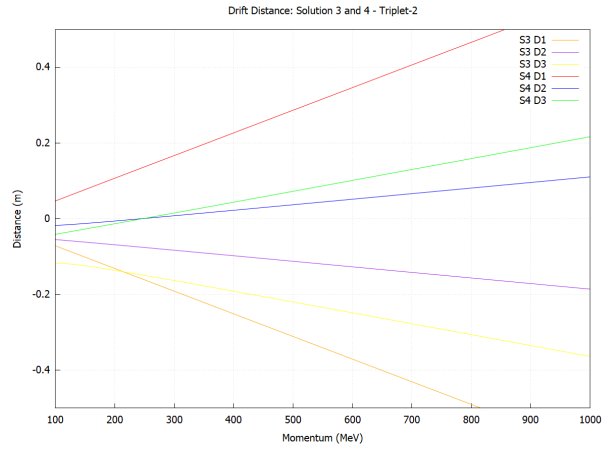


Figure 12: Drift distances: Solutions 3 & 4, Triplet-2

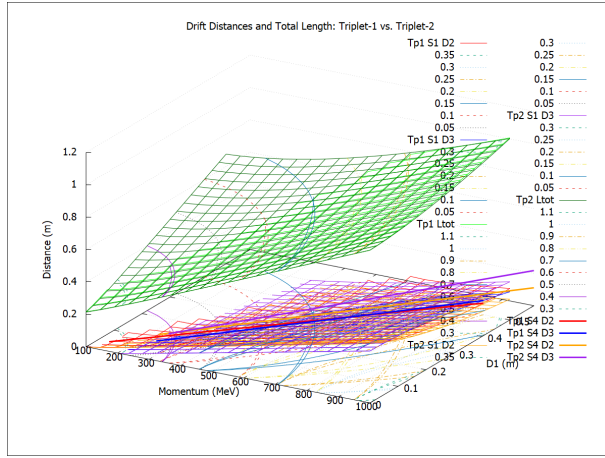


Figure 13: Drift distances and total lengths: Triplet-1 vs. Triplet-2

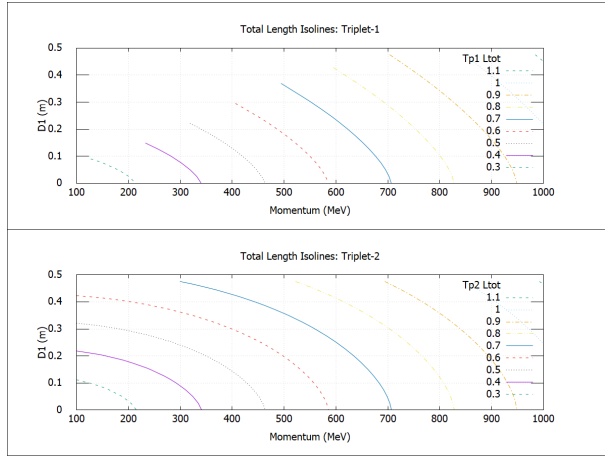


Figure 14: Isolines of total lengths

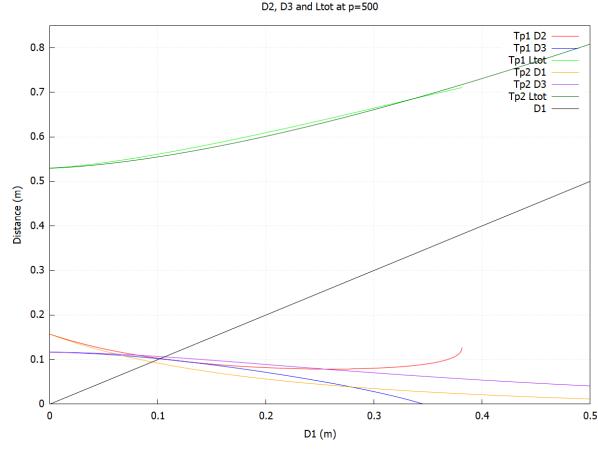


Figure 15: Drift distances at $p = 500$ MeV

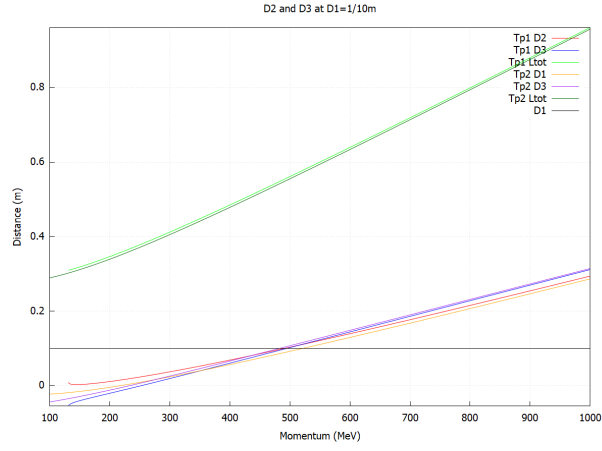


Figure 16: D_2 and D_3 when $D_1 = 0.1$ m

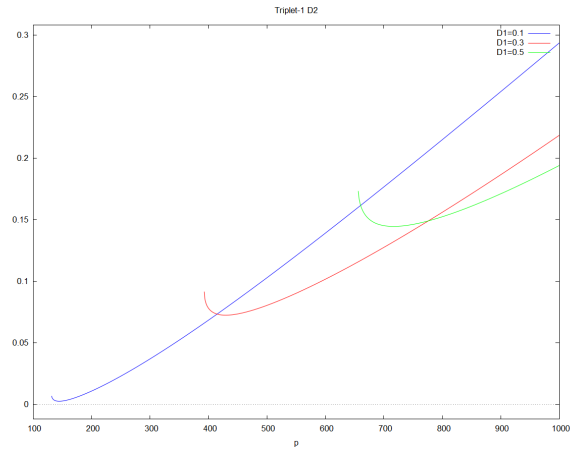


Figure 17: D_2 for Triplet-1 when $D_1 = 0.1$ m, 0.3 m and 0.5 m.

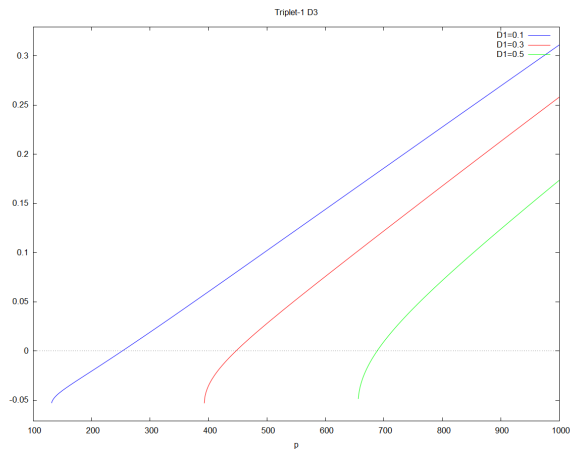


Figure 18: D_3 for Triplet-1 when $D_1 = 0.1$ m, 0.3 m and 0.5 m.

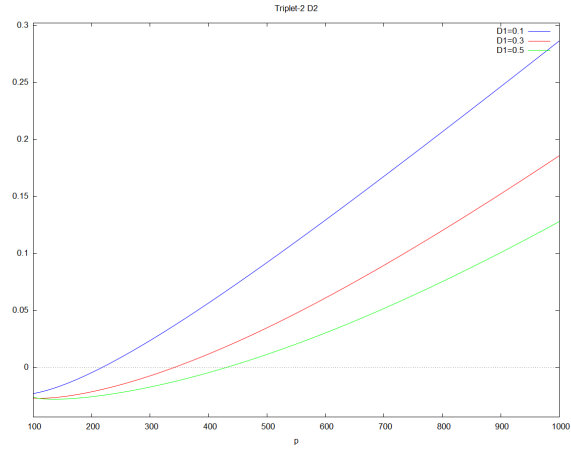


Figure 19: D_2 for Triplet-2 when $D_1 = 0.1$ m, 0.3 m and 0.5 m.

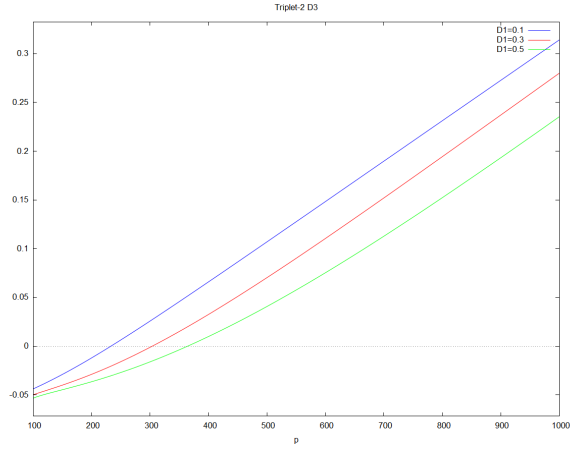


Figure 20: D_3 for Triplet-2 when $D_1 = 0.1$ m, 0.3 m and 0.5 m.